Ultrasound in Med. & Biol., Vol. 45, No. 12, pp. 3290–3297, 2019

0301-5629/$ - see front matter

https://doi.org/10.1016/j.ultrasmedbio.2019.06.410

● *Technical Note*

FOCUSED ULTRASOUND-MEDIATED HYPERTHERMIA *IN VITRO*: AN EXPERIMENTAL ARRANGEMENT FOR TREATING CELLS UNDER TISSUE-MIMICKING CONDITIONS

SARAH C. BRÜNINGK, IAN RIVENS, PETROS MOURATIDIS, and GAIL TER HAAR

Joint Department of Physics at The Institute of Cancer Research and The Royal Marsden NHS Foundation Trust, London, United Kingdom

(*Received* 14 *February* 2019; *revised* 13 *May* 2019; *in final from* 18 *June* 2019)

Abstract—An experimental arrangement that allows *in vitro* exposure of cells to focused ultrasound-mediated hyperthermia (43°C–55°C) in a tissue-mimicking phantom with biological, acoustic and thermal properties comparable to those of human soft tissue is described. Cells were embedded in a compressed collagen gel, which was sandwiched between 6-mm-thick slices of biocompatible, acoustically absorbing and thermally tissue mimicking poly (vinyl alcohol) cryo-gel. To illustrate the system's potential, cells were exposed using a 1.66-MHz focused ultrasound beam (spatial-peak temporal-average intensities (I_{SPTA}) = 900–1400 W/cm^2) that traced out a circular trajectory (5–8 mm in diameter). Real-time temperature monitoring allowed cells to be exposed reproducibly to a pre-determined thermal dose. An experimental planning tool that estimates the thermal dose distribution throughout the sample and allows spatial correlation with cell position has been developed. Treatment response was evaluated qualitatively using microscopy and cell viability testing. This experimental arrangement has significant potential for future, biologically relevant, *in vitro* focused ultrasound-mediated hyperthermia studies. (E-mail addresses: sarah.brueningk@icr.ac.uk gail.terHaar@icr.ac.uk) © **2019 The Author(s). Published by Elsevier Inc. on behalf of World Federation for Ultrasound in Medicine & Biology. This is an open access article under the CC BY-NC-ND license. (http://creativecommons.org/licenses/by-nc-nd/4.0/).**

Key Words: **Focused ultrasound, High-intensity focused ultrasound, *In vitro*, Tissue mimic, Hyperthermia.**

INTRODUCTION

High-intensity focused ultrasound (FUS), operating at ~0.5–5 MHz, and spatial peak temporal average intensities (I_{SPTA}) ≥500 W/cm^2 (ter Haar and Coussios 2007) hold great potential for cancer therapy, either as a stand-alone ablative treatment (heating to >55°C for seconds) or as a method of inducing hyperthermia (41°C–45°C for ≈1 h, with non-ablative intent) for use in combination with radiation (or chemotherapy) (Wust et al. 2002; Rao et al. 2010; Mallory et al. 2016). Recent *in vivo* studies (Martinho Costa 2017) proposed ablation of hypoxic tumour subvolumes in combination with radiotherapy, where radiosensitization caused by heat diffusion from the ablated lesions resulted in high-temperature hyperthermia (45°C–50°C for minutes) in non-ablated tumour. To exploit such promising aspects of FUS, understanding and quantifying its biological effects are essential.

Although cellular response to hyperthermia delivered by external heat sources has been studied extensively (*e.g.,* Sapareto et al. 1978; Horsman and Overgaard 2007; Lauber et al. 2015), there is less knowledge of the cellular effects of FUS exposures, and few publications address *in vitro* cell survival or cell death mechanisms. During FUS exposure, cells may be subjected to heating, mechanical stress caused by the pressure wave (alternation of compression and rarefaction), radiation force, and acoustic cavitation effects from nucleated microbubbles (Miller et al. 1996; Jernberg et al. 2001). Treatments can be tuned to enhance or suppress the relevance of each effect by judicious choice of exposure parameters. Experiments have previously been performed on cells in suspension or in 2-D monolayers (Kaufman et al. 1977; Jernberg et al. 2001; Hallow et al. 2006; Lai et al. 2006). Culture medium is, however, (i) far less attenuating than soft tissue (μ_{water} ≈ 0.02 dB/cm at 1 MHz [Culjat et al.

Address correspondence to: Sarah Brüningk, The Institute of Cancer Research, 15 Cotswold Road, SM25 NG, Sutton, UK.E-mail addresses: sarah.brueningk@icr.ac.uk gail.terHaar@icr.ac.uk

2010], $\mu_{\text{soft tissue}} \approx 0.4-0.5$ dB/cm at 1 MHz [Culjat et al. 2010; Mast 2000]); (ii) allows acoustic streaming to occur, which creates shear stresses (both (i) and (ii) restrict heating); and (iii) has acoustic cavitation thresholds dissimilar to those of *in vivo* tissues. These differences may affect cell membrane integrity, lead to cell death or render cells more vulnerable to subsequent water bath heating. Moreover, the inhomogeneous exposure of suspended cells within fluid makes it difficult to relate the biological response to quantitative exposure parameters. In monolayer cultures, radiation force may detach cells from the substrate, thus hindering spatially resolved exposure quantification, as in suspension cultures. Where cells are exposed in standard tissue culture plastics, standing waves are likely to arise from reflection at interfaces with differing acoustic impedance (*e.g.,* medium/air), inducing further uncertainty in the delivered pressure and intensity distributions. Potentially significant heating may occur as a result of sound absorption in the substrate.

To avoid these problems, cells need to be exposed to FUS within materials that are tissue mimicking in terms of biological (proliferation and adherence that is tolerant to acoustic exposure), acoustic (attenuation, speed of sound, cavitation) and thermal (thermal conductivity, specific heat capacity) properties. A good example of an *in vitro* FUS exposure system was presented by Mylonopoulou et al. (2013), who used cells embedded in agarose gels supplemented with glass microbeads to provide acoustic scattering. Although these samples were biocompatible and had acoustic properties (attenuation, speed of sound) comparable to those of human soft tissue, FUS exposures were limited to peak-to-peak pressures <5 MPa and intensities <200 W/cm^2 (1.1-MHz continuous exposures) because of the early onset of cavitation.

To the best of our knowledge, no single tissue-mimicking material meets both the biological and physical requirements described above. Hydrogels prepared from biopolymers, such as the extracellular matrix proteins collagen, fibronectin and laminin, provide excellent biological properties, but generally cannot be produced as dense, homogeneous bulk materials (*i.e.,* of centimeter dimensions) at reasonable cost (Brown et al. 2005; Abou Neel et al. 2006; Cheema and Brown 2013). This also hinders acoustic and thermal characterization (Irastorza et al. 2011). Acoustically absorbing hydrogels prepared from synthetic polymers, for example, poly(acryl amid) and poly(vinyl alcohol) (PVA), can be produced with the required volumes and acoustic properties (Kharine et al. 2003; Xia et al. 2011; Surry et al. 2018) but offer limited cell adhesion and proliferation, despite being biocompatible. We describe here an *in vitro* FUS exposure arrangement which uses a thin, compressed collagen scaffold providing the biological matrix, sandwiched between bulk PVA hydrogels. Acoustic and thermal properties of the PVA gel were characterized, and a qualitative assay of cell viability and cell distribution within the compressed collagen is described. The aim was to provide a tissue-mimicking phantom that enables the study of cellular response to FUS-mediated hyperthermia (FUS-HT) with non-ablative intent, at temperatures $<55^{\circ}C$, using peak intensities ≥ 500 W/cm^2.

METHODS

Experimental design

Figure 1a illustrates the experimental arrangement. Cells embedded in a compressed collagen gel were sandwiched between slices of 6-mm-thick PVA gel within a well of a bespoke 3-D printed well-plate (all 3-D printing material was FullCure 835, Vero White Plus, Laser Lines, Oxon, UK) consisting of six 2.8-cm-diameter, 1-cm-deep wells in a 129×86-mm frame. Each well was sealed top and bottom with individual screw-fixed 3-D printed 2.8-cm-diameter windows to which 19-μm-thick polyester film (PMX980, HiFi Industrial Film Ltd., Stevenage, UK) was attached with silicon glue (781 Acetoxy Silicone, Dow Corning, MI, USA) to provide low-absorption acoustic windows. Rubber O-rings ensured a tight seal. The sealed plate was clamped onto a horizontal holding platform within a 40-cm-deep perspex tank filled with degassed (<2 mg/mL dissolved oxygen) water at room temperature (22°C). Gels were exposed to FUS from below using a spherically focused single-element transducer (1.66 MHz, 64-mm focal length, 19.5-mm inner diameter, 63-mm outer diameter; H148-MR, Sonic Concepts, Bothell, WA, USA) mounted on a movable gantry. Water heating was prevented using a chiller (HC-100 A, Hailea, Guangdong, China). Continuous degassing was achieved using a purpose-built system based on a Liquicel (3M, Sanford, NC, USA). To mimic FUS-HT treatments, continuous wave exposures were calibrated as described previously (Civale et al. 2018) (free-field $I_{\text{SPTA}} = 200-1400$ W/cm^2 with 10% calibration uncertainty, beam dimensions of the p_{RMS}: $\text{FWHM}_{\text{transverse}} = 1.3 \pm 0.1$ mm, $\text{FWHM}_{\text{axial}} = 12 \pm 1$ mm) and were delivered by continuously moving the transducer along a 5- to 8-mm-diameter circular trajectory (positional uncertainty of ± 0.05 mm). The focal plane coincided with the collagen layer and contours were traced out for 100−300 s with a rotational speed of 1 rotation/s. These conditions represent one example of possible exposures.

As small differences in time−temperature distributions delivered correspond to large uncertainties in thermal dose (Sapareto and Dewey 1984), real-time temperature, and hence thermal dose, was monitored. A sterilized fine wire (0.1-mm diameter, 0.01-s sampling

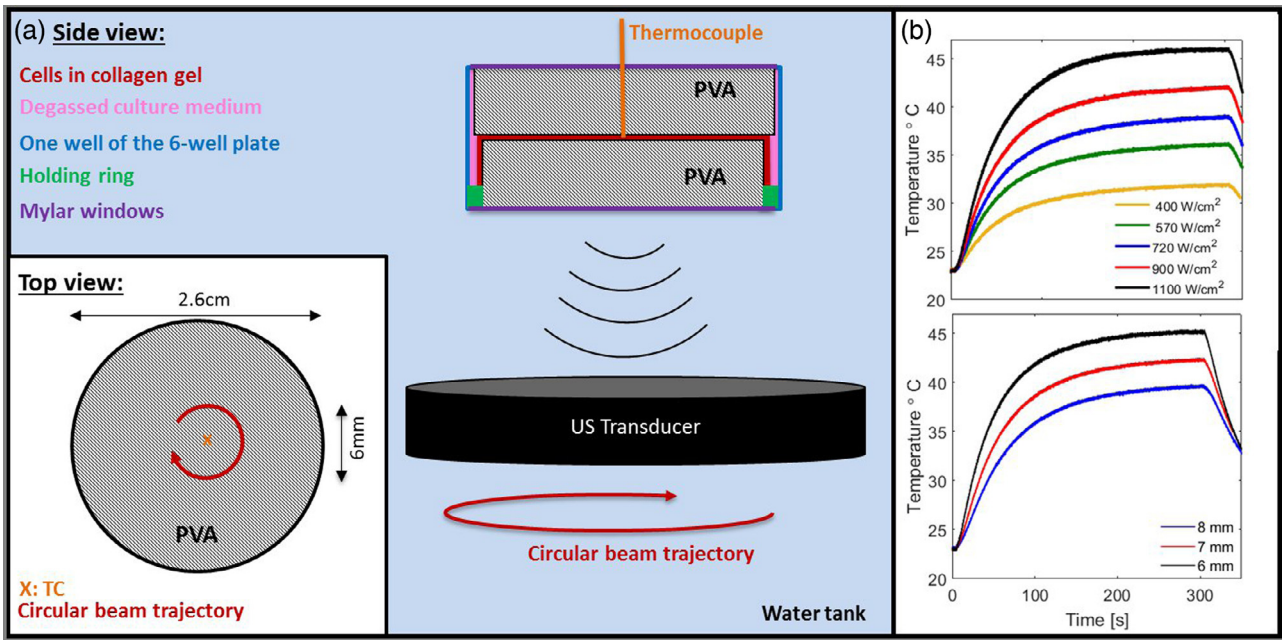

Fig. 1. (a) Schematic (not drawn to scale) of the experimental arrangement designed to enable *in vitro* FUS exposure of cells embedded in a collagen scaffold (*red*) in a tissue-mimicking environment provided by a sandwich of PVA gels (grey, 2.1 and 2.6 cm in diameter) submerged in degassed culture medium (pink, McCoy's 5A, Gibco, Paisley, UK). The collagen scaffold was held in place over the 2.1-cm-diameter PVA gel by a 3-D printed holding ring (*green*, 2.2-cm diameter). The gel sandwich was positioned within a well of a 3-D printed six-well plate (*blue*) that was sealed on both sides with 19-μm polyester film windows (*purple*) and submerged in a degassed water tank (*light blue* background). Cells were exposed to a circular FUS trajectory (see top view inset). The temperature in the collagen at the centre of the circle, was measured using a TC (orange). (b) Time–temperature profiles recorded for FUS treatments using different intensity levels (free field I_{SPTA} from 400–1100 W/cm^2, 10% calibration uncertainty) for 6-mm-diameter circular trajectories (top) and for varying diameter trajectories (bottom) at a free field I_{SPTA} of 1100 ± 110 W/cm^2. FUS exposures all started at time 0 and lasted 300 s.

rate) k-type thermocouple (TC) (5 SRTC-TT-KI-40-1 M, Omega, Manchester, UK) was inserted vertically through the top window of the sample holder and upper PVA gel, into the collagen layer. The FUS focus was localized on the TC tip using a grid of 1-s, low-acoustic-power/intensity (1.1 ± 0.1 W, 92 ± 9 W/cm^2) exposures to identify the peak temperature rise with 0.05-mm spatial precision. The circular contour exposures were then delivered with the TC at their rotational centre or at a known offset perpendicular to the beam direction. This avoided direct exposure of the TC and, thus, viscous heating artifacts. Samples could be exposed until a desired thermal dose at the centre (TD_{centre}) had been accumulated, with the FUS intensity and contour diameter determining required exposure duration (see Fig. 1b). Background noise in the temperature reading during exposure was ~0.2°C. Thermal dose was calculated based on a moving window average over 100 temperature points with upper and lower temperature envelopes used to calculate uncertainty, as previously described (Sapareto et al. 1978). It is reported in units of CEM_{43}, referring to the equivalent heating time in minutes at 43°C.

PVA gel preparation and characterization

PVA cryogels were prepared by dissolving PVA crystals (M_W 85,000–124,000 g/mol, Sigma Aldrich, Dorset, UK) at a concentration of 10% (w/w) in sterile, de-ionized, degassed water heated to 95°C and already supplemented with 5% (w/w) cellulose (Sigma Cell, Sigma Aldrich, Dorset, UK). The liquid gel was cooled for 15 min at room temperature, stirred, cast into a rectangular perspex mould (0.6 × 30 × 21 cm) and subjected to three cycles of freezing (−20°C, 5 h) and thawing (19 h) inside a timer-controlled freezer. After the last cycle, the 6-mm-thick cryogel sheet was cut into 2.1- and 2.6-cm (used for cell exposures) and 5.6-cm-diameter discs (for thermal and acoustic characterization) using custom-made cylindrical stainless steel cutters. PVA disks were sterilized by soaking for 2 h in 70% ethanol, followed by three washes in sterile phosphate-buffered saline (PBS). Gels were stored in sterile PBS for ≥18 h before use to allow them to equilibrate their water content.

Thermal conductivity and specific heat capacity were measured using a HotDisk TPS analyser (HotDisk, Gothenburg, Sweden), according to the manufacturer's

protocol, in seven independently prepared PVA samples (5.6-cm diameter). The acoustic attenuation coefficient and speed of sound were measured using the finite-amplitude-insertion-substitution method in a previously described, purpose-built experimental setup (Retat 2011) at room temperature, or 35°C, respectively.

3-D collagen cell scaffold production

All liquid reagents were degassed in a vacuum desiccator and chilled on ice. HCT116 cells (human colorectal carcinoma, obtained from the American Type Culture Collection) were grown to 80% confluence as monolayers in culture medium (McCoy's 5A, Gibco, Paisley, UK) supplemented with 10% fetal bovine serum (PAN Biotech, Dorset, UK) in a standard tissue culture incubator. Cells were gently detached using Accutase (Gibco, Paisley, UK) and concentrated to a suspension of 2.5×10^6 cells/mL in degassed complete growth medium. For preparation of a 4-mL collagen gel (Cheema and Brown 2013), 3.2 mL of rat tail collagen type I solution (2.05 mg/mL in 2% acetic acid, First Link, Birmingham, UK) was gently mixed with 0.4 mL of 10 × modified Eagle's medium (First Link) containing phenol red. The gel solution was neutralized by titration with 5 M and then 1 M sodium hydroxide; 0.4 mL of cell suspension (4°C) was immediately added and the solution was cast into one well of a standard six-well tissue culture plate (Cellstar, Greiner Bio-One International, Kremsmnster, Austria). Care was taken to prevent, or remove, visible air bubbles before polymerization for 30 min at room temperature. The polymerized gel was subjected to a confined compression under gravity in a 2.6-cm-diameter cylinder (load: 600 g, duration: 5 s), followed by unconfined compression on top of a disc of PVA gel (diameter: 2.1 cm, load: 600 g, duration: 5 s), resulting in a <1-mm-thick collagen layer. This was held in position on the PVA cryogel using a 3-D printed ring (2.2-cm diameter, 3-mm height, containing 1-mm-diameter holes to allow excess fluid to escape), and this arrangement was placed in a well of the 3-D printed six-well plate (see Fig. 1a) that was submerged in degassed culture medium (McCoy's 5A). A second PVA cryogel disc (2.6-cm diameter) was placed on the collagen scaffold. The larger diameter of this gel (2.6 cm) ensured that the collagen scaffold was completely covered by the top gel, and a small gap (1-mm radial direction) to the well walls allowed space for air bubbles and excess fluid to escape during sandwich assembly and well sealing. Collagen scaffolds were also prepared using cell suspensions which had been heated in a thermal cycler, as previously described (Brüningk et al. 2017), to thermal doses of 0, 25, 100 and 200 CEM_{43}. To minimize the cells' time in the well plate, only two wells (*i.e.,* two samples) were prepared and subsequently exposed at a time.

Treatment evaluation

After FUS exposure, collagen scaffolds were aseptically removed from the sample holder and incubated in six-well plates (Cellstar, Greiner Bio-One International) in complete growth medium supplemented with a 1% mixture of penicillin/streptomycin solution (P4333, Sigma Aldrich) and 23 μg/mL amphotericin B (A2942, Sigma Aldrich).

Three days after treatment, cell viability was assessed using MTT reagent (3-(4,5-dimethylthiazol-2-yl)-2,5-diphenyltetrazolium bromide). The samples were placed in 2 mL of fresh complete growth medium to which 0.4 mL of MTT solution (5 mg/mL MTT in sterile PBS, Sigma Aldrich) was added. Samples were incubated for 4 h and then washed three times in PBS before being fixed in 10% neutral buffered formalin solution (Sigma Aldrich) for 10 min.

As the absence of MTT staining may be due to either a lack of metabolic cell activity or the absence of cells, fluorescence staining of cell nuclei with DAPI was used to evaluate cell distributions. Formalin-fixed (optionally MTT-stained) samples were washed three times in PBS before staining with DAPI (dilution 1:1000 in PBS, Sigma Aldrich) for 10 min. Staining was followed by washing in PBS; then samples were cut into 1 × 1-cm squares and mounted on glass microscope slides in anti-fade mounting medium (H-1000, Vector Labs, Peterborough, UK). Composite images were acquired at 40 × magnification using a motorized scanning stage (Prior Scientific Instruments, Cambridge, UK) attached to a BX51 microscope (Olympus Optical, London, UK) with a CC-12 camera (Soft Imaging Systems, Muenster, Germany), driven by cellSens software (Olympus Optical). Fluorescence images were acquired using an excitation/emission wavelength of 360−370/420−460 nm filtered from a mercury burner (U-RFL-T, Olympus Optical).

Experimental planning tool

A linear acoustic model was used for FUS simulation employing the methods described in Clarke (1995) and Civale et al. (2006). The intensity distribution obtained was used to calculate dynamic temperature distributions in the gel ensemble by iteratively solving Penne's bioheat diffusion equation in its avascular form. Transducer movement was accounted for by stepping the intensity distribution along circular contours. Because not all the thermal and acoustic properties of the gel sandwich were known as the collagen layer was too thin to measure accurately, these values were adapted to match the experimentally measured time−temperature profile at the centre of the exposed ring (*i.e.,* simulation calibration). Time−temperature profiles were also recorded at 0.5-, 1.5-, 2.5- and 3.5-mm radial distance from the centre and compared

Table 1. Acoustic and thermal properties of PVA cryogel (measured) and selected human soft tissue (literature). PVA results are given as mean values +/- standard deviations calcualted over seven samples, except speed of sound, which was an average over three samples. Soft tissue data is given with uncertainties where available and was obtained from Culjat et al. (2010), Duck (1990), Mast (2000), Giering et al. (1995), Hamilton (1998) and Balasubramaniam and Bowman (1977).

Material	Λ (W m/K)	$C_{p,sp}$ (MJ/m^3/K)	μ (dB/cm at 1 MHz)	c (37˚C) (m/s)
Liver	0.564	3.62 ± 0.08	0.5	1595
Brain	0.55 ± 0.01	3.630 ± 0.001	0.6	1560
Spleen	0.543	3.592	0.4	1567
PVA gel	0.61 ± 0.05	3.0 ± 0.6	0.25 ± 0.02	1560 ± 14 (at 35˚C)

PVA = poly(vinyl alcohol); Λ = thermal conductivity; $C_{p,sp}$ = specific heat capacity under constant pressure; c = speed of sound; μ = acoustic attenuation coefficient.

with simulations performed using the calibrated tool (*i.e.,* simulation validation).

RESULTS

The PVA gel had a speed of sound and thermal properties similar to those of human soft tissues (see Table 1), although the attenuation coefficient was ~50% lower than the average for brain, liver and spleen.

In Figure 1b are representative time−temperature profiles as a function of FUS free field I_{SPTA} or of circular exposed diameter, thus demonstrating two examples of the system's flexible controllability. Both display a steep initial temperature increase that eventually plateaued before the exposure ended and cooling started. No cavitation bubble-induced mechanical damage was observed in the samples, as assessed by visual examination after exposure (visual inspection of PVA gels by eye, microscopic analysis of collagen scaffolds). However, for central temperatures $>50^{\circ}C$, structural changes in the PVA and collagen gels were palpable (softening) and visible (more transparent gel) within the exposed ring.

Figure 2a compares simulated and experimentally measured maximum temperature and total accumulated thermal dose as a function of position after simulation calibration to the central time−temperature profile. In this example, the maximum temperature variation across the heated circle was 2˚C, which translated to a thermal dose difference ≤120 CEM_{43}. Modelling based on a single calibration measurement allowed prediction of the dynamic temperature distribution throughout the collagen layer (see Fig. 2b), which can be used as an experimental planning tool for future exposures to quantify temperature and thermal dose heterogeneity across the sample.

Figure 3a and b illustrate a comparison of DAPI (blue) and MTT (gray) co-stained microscopy images of

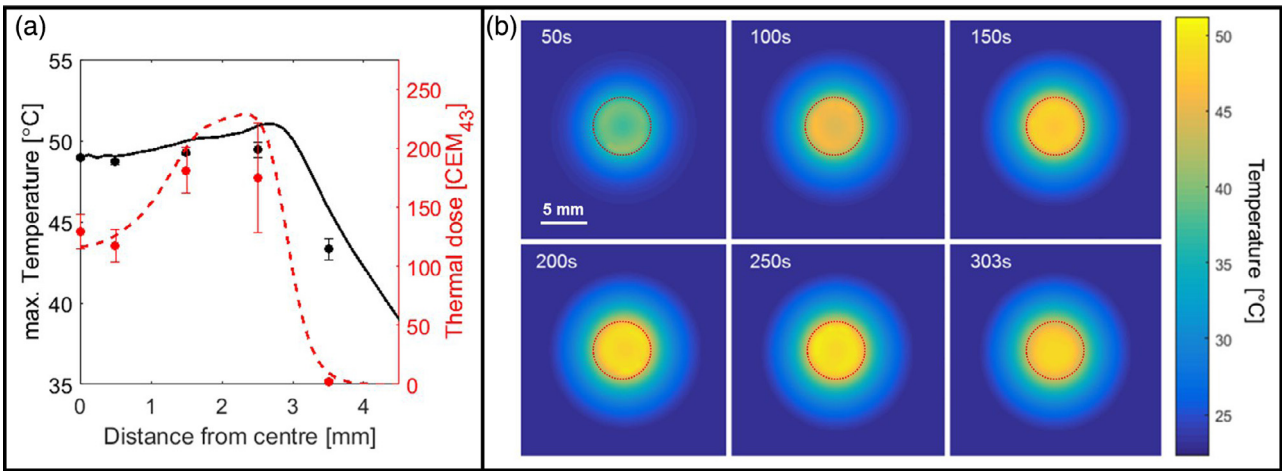

Fig. 2. (a) Comparison of simulated (*lines*) and measured (*points*) maximum temperature (*black*) and thermal dose (*red*) for 300-s exposure, free field I_{SPTA} = 1100 ± 110 W/cm^2, 6-mm trajectory diameter. The simulation was calibrated (see text) to match the temperature at the centre. Measurements at other distances from the centre represent validation data. Measurement uncertainty (variability) increased significantly as the the FUS beam approached the TC. Although maximum temperature variation within the exposed ring never exceeded 2˚C, this translates into thermal dose variations of up to 120 CEM_{43}. (b) Simulated temperature distributions through the collagen layer (within the PVA−collagen−PVA gel sandwich) at time points during and directly after the FUS exposure shown in (a). *Dashed lines* indicate transducer trajectories.

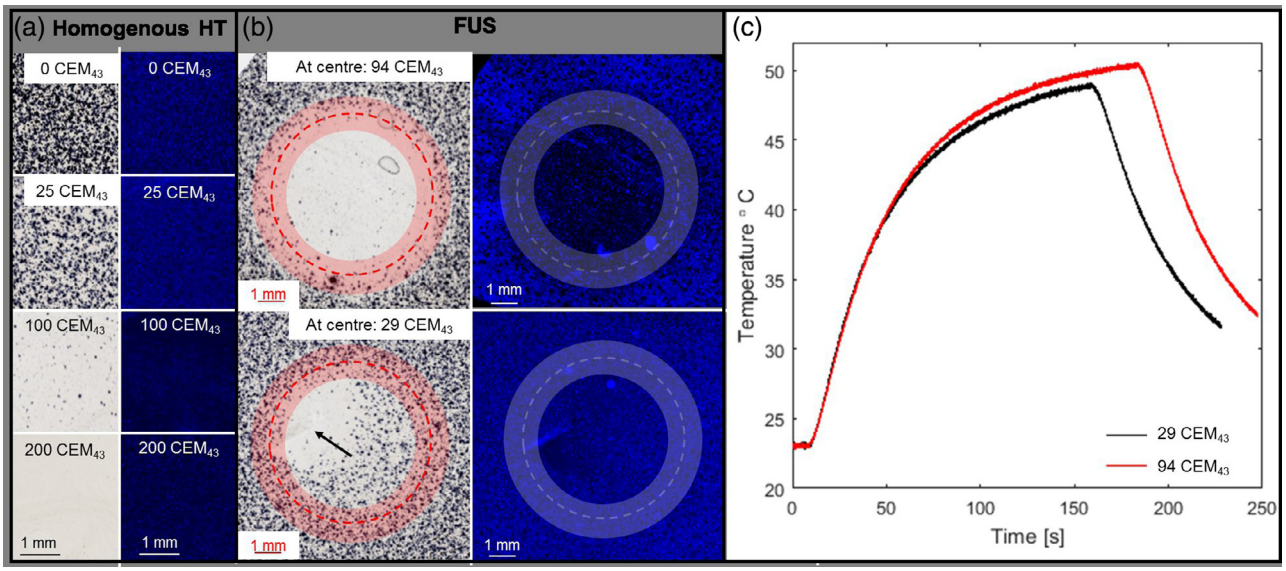

Fig. 3. (a) Microscopy images. MTT-stained brightfield images (left) and DAPI-stained fluorescence images (right) of cells heated in a thermal cycler to different thermal doses (0−200 CEM_{43}), before embedding in collagen scaffolds. (b) MTT (left)- and DAPI (right)-stained cells embedded in collagen scaffolds exposed to FUS (6 mm diameter trajectory, 1400 ± 140 W/cm^2) for two centrally measured (minimum) thermal doses of 94(84,105) CEM_{43} (top) and 29(26,33) CEM_{43} (bottom). Exposure was stopped once the desired thermal dose level was reached. All samples were stained 72 h post-exposure. Exposed trajectories are indicated by *dashed contours*; the beam full width half maximum is highlighted. A tear in the collagen gel induced by the TC and following processing was seen in the 29 CEM_{43} sample (*black arrow*). (c) Time−temperature profiles recorded by the TC for the two samples shown in (b), indicating the difference in exposure duration and similar initial temperature increase.

cells embedded in collagen gel heated either (a) in a thermal cycler or (b) by FUS-HT (29(26,33) CEM_{43} vs. 94 (84,105) CEM_{43} TD_{centre}). The central time−temperature profiles recorded for the FUS-exposed samples are provided in Figure 3c. Both evaluation assays indicated thermal dose-dependent differences while describing different aspects: MTT staining intensity, indicating cell viability, revealed agreement between the thermal cycler- and FUS-heated samples for the same thermal doses. DAPI staining (distribution of live and dead cells) revealed homogeneous distribution of cells in the TD_{centre} = 29(26,33) CEM_{43} sample and, thus, that cells were not dislocated in the scaffold by radiation force. Fewer cells were stained in the centre of the samples receiving TD_{centre} = 94(84,105) CEM_{43}, because of a lack of proliferation of heated cells relative to that of the untreated cells outside the exposed ring. The TC could cause breaks in the collagen gel that could grow because of sample handling after exposure, resulting in cell death in their direct proximity (extending several millimeters as shown in Fig. 3b, bottom row); these regions of dead cells and broken scaffold were easily identified and covered a small spatial extent in the millimeter range.

A control sham FUS-exposed sample revealed that localization of the focus on the TC tip at low intensity (free field I_{SPTA} = 92 ± 9 W/cm^2) did not cause gel breakage or reduced cell viability (not shown). Comparison of samples treated with the same TD_{centre}, using different time−temperature distributions, indicated that TD_{centre} was a good indicator of treatment efficacy and produced reproducible cell viability distributions (not shown).

DISCUSSION

A novel, flexible experimental arrangement for delivering non-ablative FUS-HT *in vitro* enabling the use of I_{SPTA} levels >500 W/cm^2 has been presented. Since there is no fundamental lower FUS intensity limit, applications for FUS-mediated drug delivery or general low-intensity ultrasound studies would also be possible. This setup offers advantages over previous ones (ter Haar et al. 1988; Mylonopoulou et al. 2013); in particular, embedding cells in a biological matrix within a bulk tissue-mimicking phantom better reproduces *in vivo* exposure conditions. Here, cells embedded within a collagen scaffold received the biological cues necessary for cell adhesion and proliferation in a 3-D culture environment that stimulates cell−cell communication and provides a tissue-mimicking cellular microenvironment (Dubessy et al. 2000; Engelhardt et al. 2010; Hu et al. 2010; Riedl et al. 2017). Although ideally FUS-HT

would be given as a homogeneous thermal dose distribution to all cells, this can rarely be realized, making it beneficial to spatially correlate cellular response with delivered thermal dose and pressure distributions. This was achieved here by robust cell embedding that prevented relocation by ultrasound radiation force while subjecting cells to simultaneous mechanical stress and heating. The use of combined MTT/DAPI staining provides a spatially resolved indication of cell viability, albeit currently in a qualitative way. However, optimization of the embedded cell concentration, time between exposure and evaluation (here fixed at 3 d), assay incubation time and evaluation of cell colony counts, rather than averaged intensities, have the potential to make the proposed assay combination quantitative.

The use of PVA cryogel discs provides FUS-HT comparable to that within human soft tissue. Although mimicking tissue with higher attenuation coefficients would be desirable, we considered the material provided a good compromise of thermal and acoustic properties, while being biologically compatible. Softening of PVA gels during heating to central temperatures $>50^{\circ}C$ could be due to a loss of cross-linking of the hydrogel in a temperature-dependent manner and thereby limit the range of usable temperatures. Future research could investigate the optimization of the PVA gel formulation to improve acoustic attenuation or the use of a different, biologically compatible bulk material.

The amount of and mechanisms for cell death after FUS-HT or water bath (or thermal cycler) heating may result from the mode of heat delivery and the additional mechanical stress induced by FUS-HT. This warrants further investigation. Using PVA gels of different formulations or different exposure parameters (trajectories, power levels and pulse rates) could allow evaluation of the relative contributions to the biological effects observed from thermal and mechanical effects. The use of gels with low acoustic attenuation coefficients could enhance mechanical effects relative to thermal ones. Using a circular exposure trajectory, most cells are indirectly heated by thermal conduction rather than direct FUS exposure. This provides an opportunity to compare heat alone with FUS-induced heating. By choosing different exposure patterns, such as spirals or rasterscans, the proportion of directly exposed cells could be altered. The proposed experimental planning tool could assist in the experimental design process to reduce the number of experiments needed. The planning tool allowed evaluation of the thermal dose distribution throughout the collagen layer. This is essential for meaningful biological response evaluation. Despite using a simple, linear propagation model, once calibrated, this was able to reproduce time–temperature profiles measured at various locations.

Use of a TC in direct contact with the cell layer posed a risk of contamination, but none was observed during this study by visual inspection. The tight, but elastic, structure of the PVA cryogel sealed the insertion channel and prevented any water ingress or leakage of medium from the well. The use of antibiotics after treatment avoided the spread of any low-level contamination.

Despite considerable advantages, the limitations of this novel arrangement include the need for real-time thermal dose monitoring with a TC and a current lack of quantitative sample analysis as discussed above. As illustrated in Figure 3b, the TC may tear the collagen layer, and these tears may be enlarged significantly upon sample handling after exposure. We speculate that this may be due to increased radiation pressure during FUS exposure, combined with heat softening of the collagen scaffold caused by a transient depolymerization of collagen fibers which renders the samples more susceptible to TC damage. Collagen breakage may be preventable using alternative temperature monitoring techniques. Ideally, these would be non-invasive and provide dynamic absolute temperature, or thermal dose, maps.

Finally, some of the experimental specifications used here did not reproduce the *in vivo* cellular microenvironment. These include the exposure at ambient temperature and the fact that cells within the scaffold were subjected to physical compression before FUS exposure. Cells were here exposed at room temperature rather than at a more physiologic $37^{\circ}C$. This ensured fast cooling once the exposure ended, thus limiting further thermal dose contributions from cooling gradients and minimizing time of cell scaffolds within the sample holder. Moreover, transducer calibration was performed at ambient temperature. It would, however, easily be possible to adapt the experimental arrangement to allow treatments at physiologic temperatures by introducing a heater to the water bath. Similarly, allowing time for cell recovery after collagen scaffold production before FUS exposure would exclude the possibility that cell sensitivity may be affected by the scaffold compression procedure. We here present only the technical feasibility of exposing cells to FUS, rather than providing biological results for a comparison of FUS and thermal cycler heating which would require more suitable biological control experiments and reliable cavitation detection measurements.

CONCLUSIONS

The experimental arrangement presented, including sample preparation, evaluation assays and planning tool, provides the framework for future *in vitro* FUS studies of the relative importance of thermal and mechanical stress resulting from non-ablative FUS-HT exposures. This setup avoids cell dislocation by radiation force, cell

exposure in a non-absorbing medium and the formation of standing waves. It provides a physiologically and thermo-acoustically tissue-mimicking environment that can be exposed to intensity levels approaching those used for *in vivo* FUS treatments.

Acknowledgments—We acknowledge NHS funding to the NIHR Biomedical Research Centre at The Royal Marsden and The Institute of Cancer Research. Research at The Institute of Cancer Research is supported by Cancer Research UK under Program C33589/A1972. The work of S.B. was funded by Cancer Research UK under S1456.

Conflict of interest disclosure—The authors declare no competing interests.

REFERENCES

Abou Neel EA, Cheema U, Knowles JC, Brown RA, Nazhat SN. Use of multiple unconfined compression for control of collagen gel scaffold density and mechanical properties. Soft Matter 2006;2: 986–992.

Balasubramaniam T, Bowman H. Thermal conductivity and thermal diffusivity of biomaterials: A simultaneous measurement technique. J Biomech Eng 1977;99:148–154.

Brown BRA, Wiseman M, Chuo CB, Cheema U, Nazhat SN. Ultrarapid engineering of biomimetic materials and tissues: Fabrication of nano- and microstructures by plastic compression. Adv Funct Mater 2005;15:1762–1770.

Brüningk SC, Ijaz J, Rivens I, Nill S, ter Haar G, Oelfke U. A comprehensive model for heat-induced radio-sensitisation. Int J Hyperthermia 2017;34:1–11.

Cheema U, Brown RA. Rapid fabrication of living tissue models by collagen plastic compression: Understanding three-dimensional cell matrix repair. In Vitro 2013;2:176–184.

Civale J, Clarke R, Rivens I, ter Haar G. The use of a segmented transducer for rib sparing in HIFU treatments. Ultrasound Med Biol 2006;32:1753–1761.

Civale J, Rivens I, Shaw A, ter Haar G. Poly(vinyl alcohol) cryogel phantoms for use in ultrasound and MR imaging. Phys Med Biol 2018;63 055015.

Clarke RL. Modification of intensity distributions from large apertature ultrasound sources. Ultrasound Med Biol 1995;21:353–363.

Culjat MO, Goldenberg D, Tewari P, Singh RS. A review of tissue substitutes for ultrasound imaging. Ultrasound Med Biol 2010;36: 861–873.

Dubessy C, Merlin JL, Marchal C, Guillemin F. Spheroids in radiobiology and photodynamic therapy. Crit Rev Oncol/Hematol 2000;36: 179–192.

Duck FA. Physical properties of tissue: A comprehensive reference book. New York: Academic Press; 1990.

Engelhardt E, Stegberg E, Brown RA, Hubbell JA, Wurm FM, Adam M. Compressed collagen gel: A novel scaffold for human bladder cells. J Tissue Eng Regen Med 2010;4:123–130.

Giering K, Lamprecht I, Minet O, Handke A. Determination of the specific heat capacity of healthy and tumorous human tissue. Thermochim Acta 1995;251:199–205.

Hallow DM, Mahajan AD, McCutchen TE, Prausnitz MR. Measurement and correlation of acoustic cavitation with cellular bioeffects. Ultrasound Med Biol 2006;32:1111–1122.

Hamilton G. Investigations of the thermal properties of human and animal tissues. Ph.D. thesis: University of Glasgow; 1998.

Horsman MR, Overgaard J. Hyperthermia: A potent enhancer of radiotherapy. Clin Oncol 2007;19:418–426.

Hu K, Shi H, Zhu J, Deng D. Compressed collagen gel as the scaffold for skin engineering. Biomed Microdevices 2010;12:627–635.

Irastorza RM, Achilli M, Amadei M, Blangino E, Drouin B, Mantovani D. Ultrasonic setup for testing hydrogels: Preliminary experiments on collagen gels. Adv Mater Res 2011;409:146–151.

Jernberg A, Edgren MR, Lewensohn R, Wiksell H, Brahme A. Cellular effects of high-intensity focused continuous wave ultrasound alone and in combination with X-rays. Int J Radiat Biol 2001;77: 127–135.

Kaufman GE, Miller MW, Dan Griffiths T, Ciaravino V, Carstensen EL. Lysis and viability of cultured mammalian cells exposed to 1 MHz ultrasound. Ultrasound Med Biol 1977;3:21–25.

Kharine A, Manohar S, Seeton R, Kolkman RGM. Poly(vinylalcohol) gels for use as tissue phantoms in photoacoustic mammography. Phys Med Biol 2003;48:357–370.

Lai CY, Wu CH, Chen CC, Li PC. Quantitative relations of acoustic inertial cavitation with sonoporation and cell viability. Ultrasound Med Biol 2006;32:1931–1941.

Lauber K, Brix N, Ernst A, Hennel R, Krombach J, Anders H, Belka C. Targeting the heat shock response in combination with radiotherapy: Sensitizing cancer cells to irradiation-induced cell death and heating up their immunogenicity. Cancer Lett 2015;368:209–229.

Mallory M, Gogineni E, Jones GC, Greer L, Simone CB. Therapeutic hyperthermia: The old, the new, and the upcoming. Crit Rev Oncol/Hematol 2016;97:56–64.

Martinho Costa MF. Preclinical investigation of combined focused ultrasound and radiotherapy to improve tumour response to treatment. Ph.D. thesis: University of London; 2017.

Mast TD. Empirical relationships between acoustic parameters in human soft tissues. Acoust Res Lett 2000;7853:37–42.

Miller MW, Miller DL, Brayman AA. A review of in vitro bioeffects of inertial ultrasonic cavitation from a mechanistic perspective. Ultrasound Med Biol 1996;22:1131–1154.

Mylonopoulou E, Bazán-Peregrino M, Arvanitis CD, Coussios CC. A non-exothermic cell-embedding tissue-mimicking material for studies of ultrasound-induced hyperthermia and drug release. Int J Hyperthermia 2013;29:133–144.

Rao W, Deng ZS, Liu J. A Review of Hyperthermia Combined With Radiotherapy/Chemotherapy on Malignant Tumors. Crit Rev Biomed Eng 2010;38:101–116.

Retat L. Characterisation of the acoustic, thermal and histological properties of tissue required for high intensity focused ultrasound (HIFU) treatment planning. Ph.D. thesis: University of London; 2011.

Riedl A, Schlederer M, Pudelko K, Stadler M, Walter S, Unterleuthner D, Unger C, Kramer N, Hengstschläger M, Kenner L, Pfeiffer D, Krupitza G, Dolznig H. Comparison of cancer cells in 2D vs. 3D culture reveals differences in AKT-mTOR-S6 K signaling and drug responses. J Cell Sci 2017;130:203–218.

Sapareto SA, Dewey WC. Thermal dose determination in cancer therapy. Int J Radiat Oncol Biol Phys 1984;10:787–800.

Sapareto SA, Hopwood LE, Dewey WC, Raju MR, Gray JW. Effects of hyperthermia on survival and progression of Chinese hamster ovary cells. Cancer Res 1978;38:393–400.

Surry K, Austin H, Fenster A, Peters TM. Focused ultrasound transducer spatial peak intensity estimation: A comparison of methods. Phys Med Biol 2018;63:5529–5546.

ter Haar G, Coussios C. High intensity focused ultrasound: Past, present and future. Int J Hyperthermia 2007;23:85–87.

ter Haar G, Walling J, Loverock P, Townsend S. The effect of combined heat and ultrasound on multicellular tumour spheroids. Int J Radiat Biol 1988;53:813–827.

Wust P, Hildebrandt B, Sreenivasa G, Rau B, Gellermann J, Riess H, Felix R, Schlag PM. Review: Hyperthermia in combined treatment of cancer. Lancet Oncol 2002;3:487–497.

Xia W, Piras D, Heijblom M, Steenbergen W, van Leeuwen TG, Manohar S. Poly(vinyl alcohol) gels as photoacoustic breast phantoms revisited. J Biomed Opt 2011;16 075002.